# MECHANICAL FATIGUE SIMULATION TESTING OF FUEL BUNDLES AND SPECIMENS FOR END PLATE FAILURE

Michael Gabbani, Tim Richards, A.M. Babayan, E.G. Price

AECL CANDU 2251 Speakman Drive Mississauga, Ontario Canada L5K 1B2

#### ABSTRACT

In November of 1990, normal refuelling operations at the Darlington Nuclear Generating Station Unit 2 (DNGS2) were prevented by fuel bundle failure at the outlet end of channel N12. Subsequent inspections revealed that a number of high-powered channels had end plate cracks on the outlet fuel bundles predominantly initiating at the notch formed by the weld between the end plate and the fuel pencil end caps. To identify the cause of fuel bundle failure, a multi-disciplined investigation was launched into the problem.

As examinations on the failed fuel bundles in the hot cells at Chalk River Laboratories later confirmed fatigue as the mechanism causing end plate failure, an experimental out-reactor program was conducted to investigate the response of fuel bundles under dynamic loading conditions. The objective of the program was to identify whether axial and/or lateral vibration of fuel elements could contribute to end plate (fatigue) failure and if so which of the two is the likely mode causing end plate failure observed at DNGS2.

The room temperature axial bundle fatigue tests conducted in this experimental program produced through wall end plate failures. The end plate fractures were associated with the welds and the point of initiation appeared to be at or near the tip of the weld notch between the end cap spigot and end plate. Fracture surface examination revealed some similarities to the field failures, however distinct differences were noted in fracture location on the end plates and the presence of a "Black Eye" fracture pattern associated with most DNGS2 failures.

Results from the lateral vibration tests were also similar to field failures; however significant differences existed in the amount of fretting and the higher degree of secondary cracking associated with the tests compared to field failures.

The results from the tests indicated that both axial and transverse bundle vibrations can cause end plate (fatigue) failure. However, the tests were unable to duplicate all of the fracture features unique to the DNGS2 failures. It is conceivable that the inability to accurately reproduce in-reactor conditions particularly mode of hydraulic loading, contributed to the marked differences in fractures.

#### 1. INTRODUCTION

On November 30, 1990, a refuelling operation wa attempted on channel N12 of the Unit 2 reactor of the Darlington Nuclear Generating Station. The fuel carrier carrying two fuel bundles, jammed on insertion into the outlet end fitting and only with difficulty was it removed a month or so later. Subsequent examination in the fuel bay showed fragments of fuel element and end plate amongst the intact bundles that were to have been inserted into N12.

An in-situ examination on a number of fuel channels using a television camera revealed more outlet position bundles with cracked end-plates. Eventually, eight channels in the columns 12 and 13 were identified as having cracked fuel bundles. The results of the above survey initiated a metallurgical investigation into the mechanism of cracking to support the multi-discipline investigation conducted by the Darlington project to determine the basic cause.

Examination of the failed end plates at AECL-CRL later showed that fatigue was the cause of failure and fatigue initiation primarily occurred in the notch between the end plate and the end cap of the fuel pencil. Low amplitude high cycle fatigue was identified as the likely mechanism of end plate failure and out-reactor experimental test programmes at OHRD, AECL-CRL, and AECL-CANDU were devised to separate the effects of axial and lateral deflections on the failures at DNGS-2.

In the test programs, representative end plate to end cap welds were cyclically loaded in directions parallel and transverse to the fuel pencil axis and in an autoclave in order to determine the fatigue resistance of the weld while cyclic axial tests were conducted on complete bundles at R.T.

This paper presents the results of tests examining the effects of transverse pencil vibration and the performance of bundles under axial cyclic loads applied mechanically.

# 2. MODE OF OPERATION OF DARLINGTON FUEL BUNDLES

Each fuel channel in a Darlington reactor contains thirteen fuel bundles. At the outlet end, the #1 bundle is held in place by a 4 segment latch which supports most of the elements in the outer ring of the bundle. This outlet bundle carries the hydraulic load imposed on the thirteen bundle string by flows of up to 28 kg/s of heavy water.

The flexibility of the end plate allows the centre elements to move in the axial direction with respect to the outer elements. The end plate deflects elastically from hydraulic loads and permanent deflection occurs by creep. Towards the outlet end this creep deflection is enhanced by transfer of some of the hydraulic load on the fuel string through the contacting end plates.

The described operating condition has not led to any problems in the Bruce reactors, but in early operation of the Darlington Unit 2 reactor which has generally higher in-channel flows, end plate failures occurred.

#### 3. OBJECTIVE OF THE EXPERIMENTAL PROGRAMME

The programme of fatigue testing to determine the properties of end plate to end cap joints under conditions simulating end plate deflection was carried out by Ontario Hydro Research Division and is reported in a separate paper. However, another mode of vibration i.e. transverse element deflection is possible and the parameters of amplitude of deflection against cyclic life were explored in this investigation to see if such motions could be the cause of failure.

At AECL-CANDU, two lateral fatigue test programmes were undertaken. On one, fuel elements with end plates attached were cut from production fuel bundles so that element deflection would stress the end plate to end cap weld closest to the region of the end plate where the radial ribs and intermediate circumferential web intersect. This position was a prime location for failures in field failures. On the second, three half length elements were welded to a strip to simulate the joints on the outer and intermediate rings of the end plate.

Tests, in which cyclic axial loads were applied to actual fuel bundles supported against a simulated latch, were undertaken to see if the cyclic life predicted from the small specimen program would be sustained by a bundle loaded as described, and if cracking occurred in the positions and patterns seen in the field failures. On one test the crack progression was monitored to confirm predictions that crack initiation occurred early in life for stressing above the fatigue threshold.

#### 4. EXPERIMENTAL DETAILS

Details for each of the three types of fatigue experiments are described below.

#### 4.1 Axial Bundle Fatigue Tests

The general arrangement of the test set-up for the axial bundle fatigue tests is shown in Figure 1.

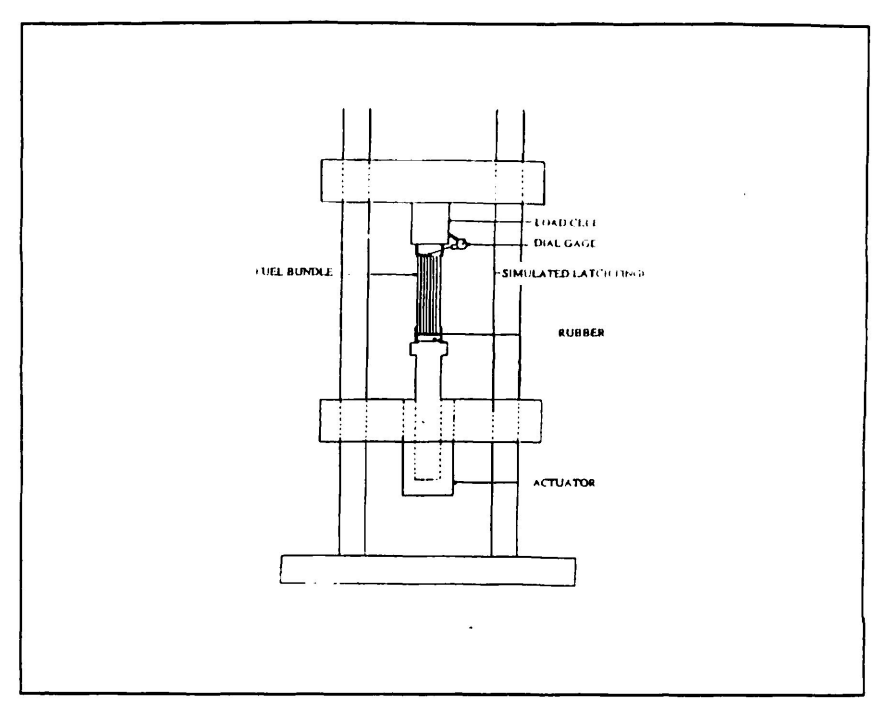


FIGURE 1: Schematic of set-up for axial bundle fatigue tests

Unirradiated fuel bundles were cycled to failure (detectable end -plate cracks) under load control in an Instron load frame. The top end of the bundle (simulated downstream end of bundle 1) was held tight against a latch with the same latch to pencil 18 orientation that was seen on the failed outlet bundle in channel Q12 of DNGS-2. The upstream end plate was supported by urethane pads which were used to distribute the load across the end-plate in an attempt to simulate hydraulic loading.

Three tests were performed:

#### 4.1.1 Test 1.

In Test 1, the bundle was supported by a 3.2 mm thick pad of 75 Shore A hardness on a 50 mm thick pad of 25 Shore A hardness. The bundle was cycled between 3 kN and 5.5 kN at 1 Hz. The loads were higher than those expected in reactor.

#### 4.1.2. Test 2.

Test 2 was a repeat of Test 1 except that ultrasonic (U.T.) inspection was used to periodically detect and monitor crack growth. The ultra-sonic examination inspection was performed by OHRD.

#### 4.1.3. Test 3.

Test 3 was a simulation of the normal flow conditions in a Darlington channel. Work on the ETR-7 rig at AECL-SPEL established the relative deflections of the inner and intermediate rings on the downstream end plate of bundle 1 under 30 kg/s flows and the

deflection on the central element (pencil 37) at flows between 28 kg/s and 32 kg/s. By using four, 25 mm thick pads of 80 Shore A hardness, these deflections could be simulated on the load frame. The bundle was cycled between loads of 2.6 kN and 3.8 kN at 10 Hz.

# 4.2 Transverse Vibration Tests (Type A) on Single and Three Pencil Samples

The general arrangement of the test set-up is shown in Figure 2. The deflection amplitude at the fuel element mid-length was set by adjusting the amount of eccentricity on the drive shaft experienced by a rod connected to the shaft by a swivel joint and to the fuel pencil through a clamp at the other end. For the three element samples, the clamp was positioned around the central element and only this element was cycled. The vibration frequency was controlled by the motor speed. To ensure a realistic specimen geometry, the test specimens used were fuel elements cut from production fuel bundles with sections of end plates attached. Two clamping plates were bolted to the support frame as shown in Figure 2. These plates were designed to support, rigidly, the end plate portion of the sample. A typical clamping arrangement for a three element sample is shown in Figure 3. Figure 4 shows the clamp used at element mid-length for lateral displacement.

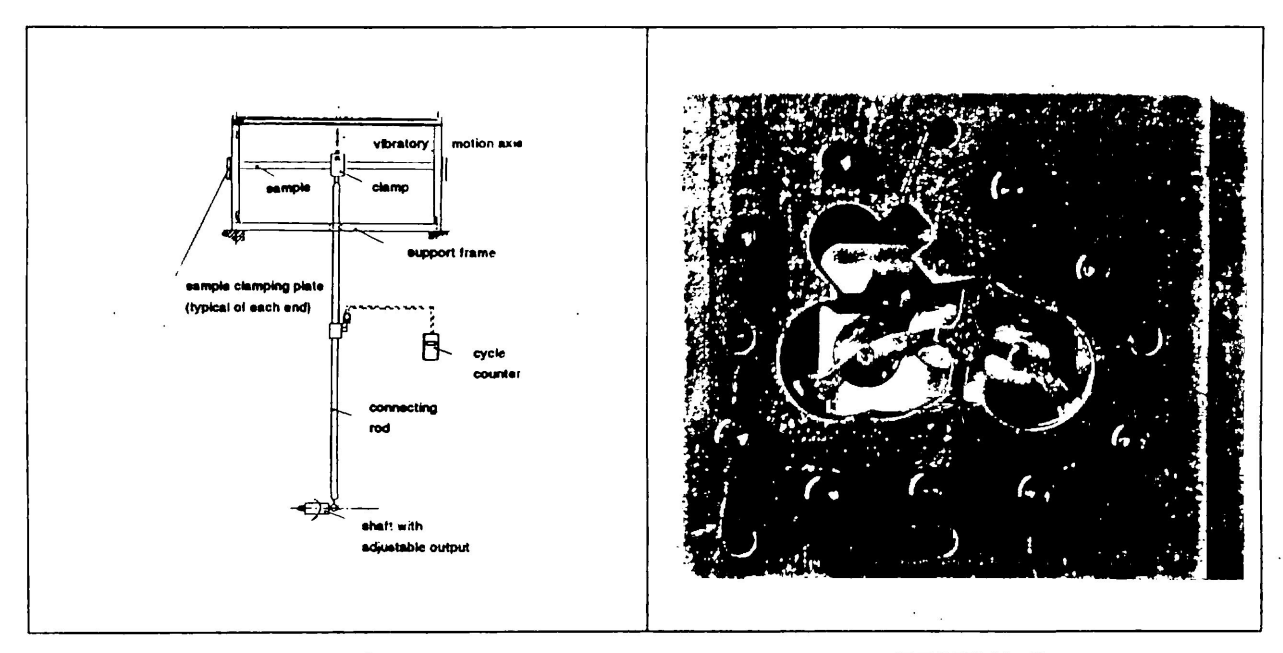


FIGURE 2: Set-up for TYPE A lateral fatigue tests

FIGURE 3: Support arrangement for TYPE A samples

Tests were conducted at (element mid-span) displacements of between  $\pm$  0.5 mm and  $\pm$  3 mm. In some of the tests a static deflection on selected "webs" of the end plate portion of the sample was applied. The purpose of this was to simulate the deflection of the end plate

caused by the hydraulic drag forces at bundle position # 1.

In the series of experiments, elements were vibrated either in the circumferential direction or in the radial direction with reference to the fuel bundle end plate.

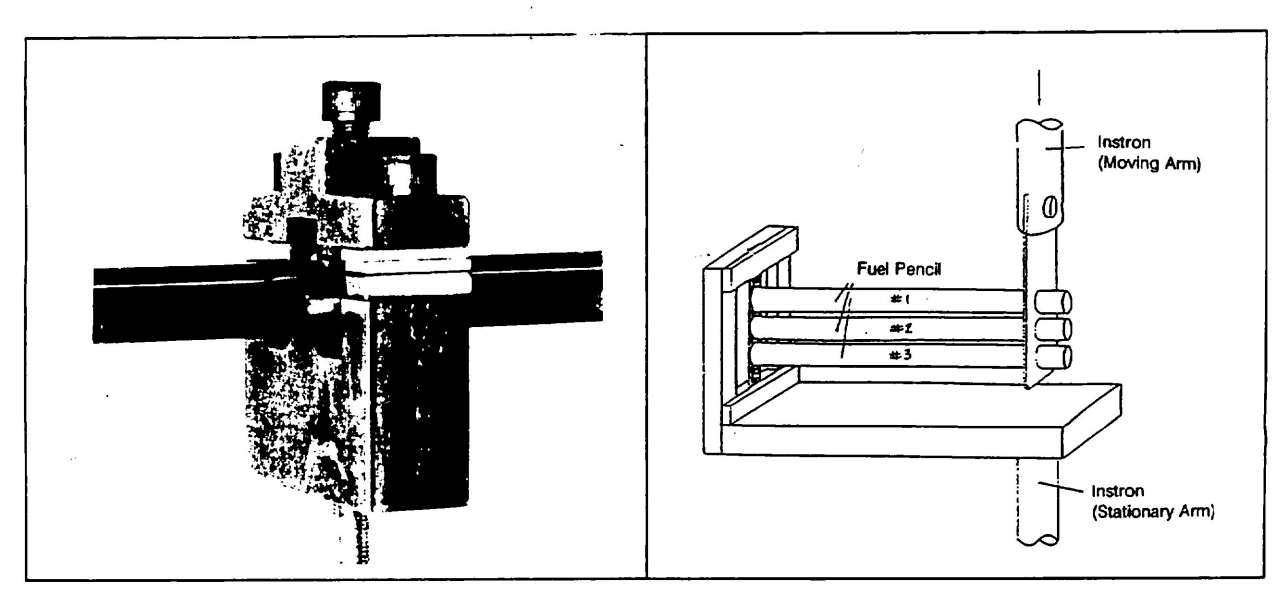


FIGURE 4: Clamping arrangement for TYPE A lateral fatigue specimens

FIGURE 5: Set-up for TYPE B lateral fatigue tests

#### 4.3. Transverse Vibration Tests (type B) on Three Element Samples

The specimens for this test were specifically produced for this test and were meant to simulate (using straight rather than curved end plate material) the pencils on the outer ring. Each specimen consisted of hollow pencils welded to a strip punched from Zircaloy-4 sheet in the same material condition as production end plates with the strip axis perpendicular to the rolling direction of the sheet stock. The fuel pencils were spot-welded to the strip material at GE Canada, according to the standard practice for bundle assembly.

The testing jig (shown in Figure 5) was driven by an Instron servohydraulic testing machine. Tests were conducted at amplitudes of  $\pm$  1 to  $\pm$  3 mm and at frequencies of 4 to 10 Hz.

Constant amplitude tests were run to establish the fatigue behaviour for the given specimen geometry. Varying load/amplitude tests were performed to see whether fracture features such as the "black eye" initiation regions and beachmarks, observed in DNGS2 field failures, could be reproduced through transverse fuel element vibration.

#### 5. RESULTS

The results from the different experiments are presented under the following subsections.

#### 5.1 Axial Bundle Fatigue Tests

### 5.1.1 Cyclic Life

A summary of test conditions and results is listed in Table 1. In Test 1, through wall cracks were produced on both end plates between 73,000 and 130,000 total cycles. Through wall cracks were produced in the second test after 61,000 cycles. Resonance in the hydraulic lines of the load cell likely decreased the time to failure of the second test. The ultrasonic examinations, (UT) which were conducted at least every 10,000 cycles initially detected cracks in the period between 30,000 and 40,000 cycles.

Two cracks were detected by U.T. in Test 3 after  $5\times10^6$  cycles. No through wall cracks were detected after  $10\times10^6$  cycles and the test was stopped. A U.T. inspection at this time did not reveal any further cracking.

TABLE 1:
Results from the Axial Bundle Test Program

Test No.	Load Amplitude (kN)	Deflection Amplitude (mm)	Observations
1	4.25 ±1.25	1.0 ±.29	Failure through the end plate between 80,000 and 130,000 cycles.
2	4.25 ±1.25	1.0 ±.29	Failure after 63,000 cycles through end plate
3	3.20 ±.60	.55 ±.06	Partial through end plate cracks after 5 million cycles

#### 5.1.2 Crack Development

The first two tests produced a significant proportion of cracks on the outer ring of the downstream end plate which is inconsistent with in-reactor failures. This skew in crack distribution is likely a result of the load distribution produced by the pad configuration used in these first two tests. The middle ring of the end plate (both ends) is the preferred crack location in reactor and this was also seen in the three axial bundle tests despite the relatively high number of cracks on the outer ring in the first two tests (see Figure 6 for Test 2).

A crack growth curve (Figure 7) was developed from the periodic

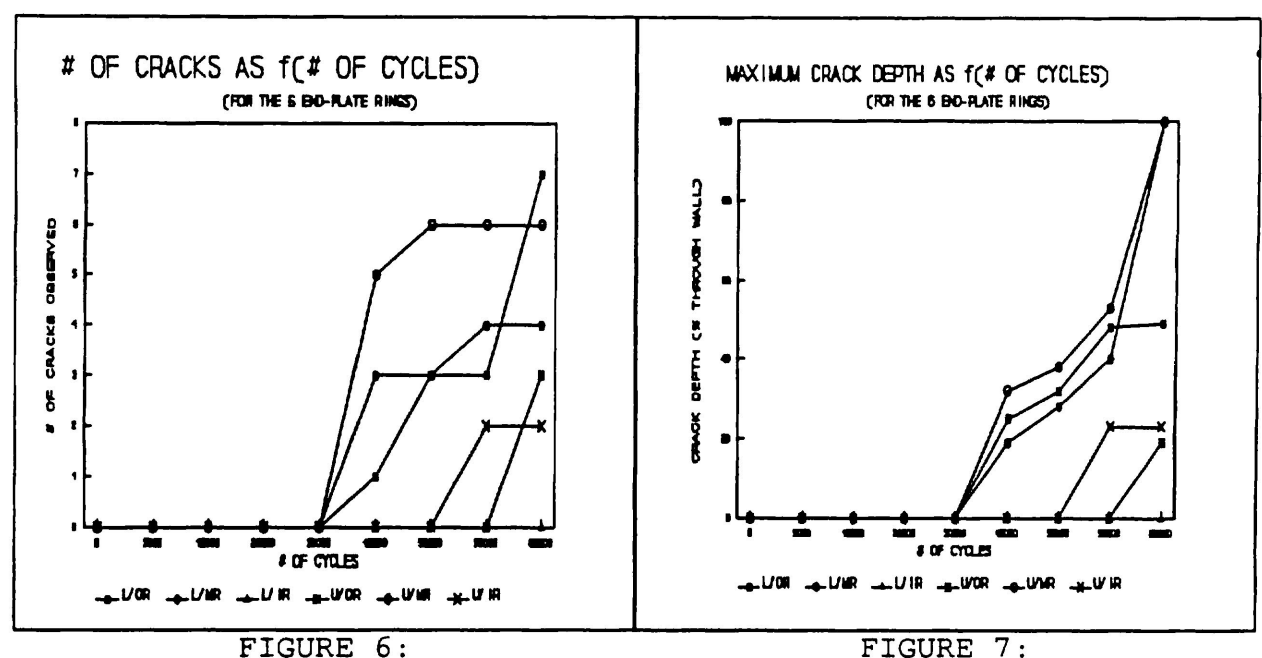
U.T. scans. The propagation rates for all cracks were quite similar and indicative of the rapid progression phase of fatigue.

#### 5.1.3 Fractography

The cracks produced in these tests were smooth with little surface roughness, very similar to those produced in reactor. The measured fatigue striation spacings were similar to those measured on cracks taken from reactor.

The two most prominent features on in-reactor cracks, beachmarks and "black eyes", were not reproduced in the axial bundle tests. The constant amplitude room temperature axial loading would not be expected to produce these effects.

The fine features (as viewed at >1000 X magnification under the Scanning Electron Microscope) observed on cracks produced in the first two tests were less brittle in appearance than those produced on in-reactor cracks, consistent with higher stresses being used in the simulation tests. The incipient cracks produced in TEST 3 could not be opened up for examination.



Distribution of cracks in the end plate during TEST 2.

Approximate crack growth rates measured in TEST 2

# 5.2 Transverse vibration tests (type A) on one and three element samples

### 5.2.1 Single Element Tests

Table 2 lists the results from the test program. The first three single element specimens tested at  $\pm$  3 mm failed through the weld between the end-plate and the end cap. The number of cycles to failure ranged from 22,000 up to 230,000. Specimens were deflected in axes either parallel to the radial web or to the circumferential ring: based on the limited data, there was no obvious difference in fatigue life.

An additional single element test (test 4) conducted at a lower deflection amplitude (±1mm) resulted in failure through the end plate initiating in the weld notch between the end cap and end plate. For this test an axial deflection was imposed on one web of the end plate sample. This was done to simulate the elastic deflection induced by hydraulic drag on the outlet bundle end plate. No cracks were reported at the weld on the other end of the specimen where no end plate pre-strain was applied.

#### 5.2.2 Three Element Tests

Further tests were conducted on three element samples (tests 5,6,7 and 8) which resulted in failures through the end plate. Test #5, cyclically deflected in the radial direction at a deflection amplitude of ±1mm, resulted in end plate failure after 5 million cycles. For this test both ends of the sample were pre-strained and cracks were found on both end plates. Test #6, cyclically deflected in the radial direction at a deflection amplitude of ±2mm failed after 1 million cycles. For this test both ends of the sample were also pre-strained and similar crack observations as in test 5 were noted. However, the smaller of the two cracks travelled predominantly through the weld rather than through wall.

In tests #7 and #8 the amplitude of deflection was  $\pm 1.5 mm$  and  $\pm .5 mm$  respectively. Both tests produced failures through the end plate. Again in Test #7 the smaller of the two cracks, a partial crack progressed through the weld rather than through wall. Test #7 resulted in failure after 2.5 million cycles while test #8 resulted in failure after 23 million cycles.

Although the surfaces were macroscopically smooth, they appeared rougher than the cracks produced in the axial bundle tests and in reactor. Features such as striations were present but generally difficult to detect.

The number of cycles to failure for single and 3-element (type A) lateral tests are shown in figure 8.

TABLE 2: Results from Type A lateral deflection tests

Test No.	Sample Type	Test Dir. (w.r.t end plate)	Amplitude (mm)	Deflection (end plate dome) (mm)	Observations
1	Single el.	Tangential	±3	0	Fail. through the weld after 230,000 cycles
2	Single el.	Tangential	±3	0	Fail. through the weld after 64,000 cycles
3	Single el.	Radial	±3	0	Fail. through the weld after 22,000 cycles
4	Single el.	Radial	±1	. 64	Fail. through the end plate after 10 million cycles
5	Three el.	Radial	±1	. 64	Fail. through the end plate after 5 million cycles
6	Three el.	Radial	±2	. 64	Fail. through the end plate after 1 million cycles
7	Three el.	Radial	±1.5	. 64	Fail. through the end plate after 2.5 million cycles
8	Three el.	Radial	±.5	. 64	Fail. through the end plate after 23 million cycles

# 5.3 Transverse vibration tests (type B) on three element samples

# 5.3.1 Constant Amplitude Tests.

A single crack originated from the weld fissure of fuel pencil #1 and penetrated through the strip. The number of cycles to failure for each test amplitude is given in Table 3 below. The fracture faces had a macroscopically smooth appearance. Surface ridges, perpendicular to the direction of crack propagation, were observed indicating multiple crack initiation points from the weld fissure.

Test ID	Mode of E/P Stressing	Frequency (Hz)	Amplitude (±mm)	No. of cycles at each amp/freq	No. of cycles to failure	Surface roughness (µm)
1	Constant amplitude	10	1	-	1.33 x 106	2.07
2	Constant amplitude	6	2	-	>350,000	2.06
3	Constant amplitude	4	3	-	12,719	1.47
4	Variable deflection amplitude	4	3 1	5,000 10,000	63,719	1.57
5	Variable loading frequency	4	3	2,000 2,000	46,626	1.66
6	Variable frequency and amplitude	6 4 10 4	2 3 1 3	10,000 5,000 100,000 5,000	749,000	Oxide Film prevented analysis

(1.) roughness is defined as the average amplitude of the hills and valleys of a surface profile from the computed mean.

Metallographic examination of the weld cross-section showed that cracking had originated in the transformed beta region of the endplate and propagated along the weld profile through the fine-grain prior beta grains. Towards the centre of the weld the crack changed direction and broke through the base metal.

Scanning Electron Microscope (SEM) examination of the fractures showed striation-like features in the weld metal near the initiation region and in the base metal. Average striation spacing was approximately 0.4-0.5  $\mu m$ . Large secondary cracks, perpendicular to crack propagation direction, were observed. A large number of finer secondary cracks were also present.

#### 5.3.2 Variable Amplitude/Frequency Tests.

The macroscopic appearance of the fracture surfaces as well as crack profile and surface roughness were similar to those observed in constant amplitude tests. Distinct beachmarks, as observed in some end plate field failures were not observed in Tests #4 and #5. Some faint bands could be observed, but it is not clear that these bands were due to changes in loading history. In test #6 (variable amplitude and frequency), two cracks had originated at the weld fissures of the outer pencils.

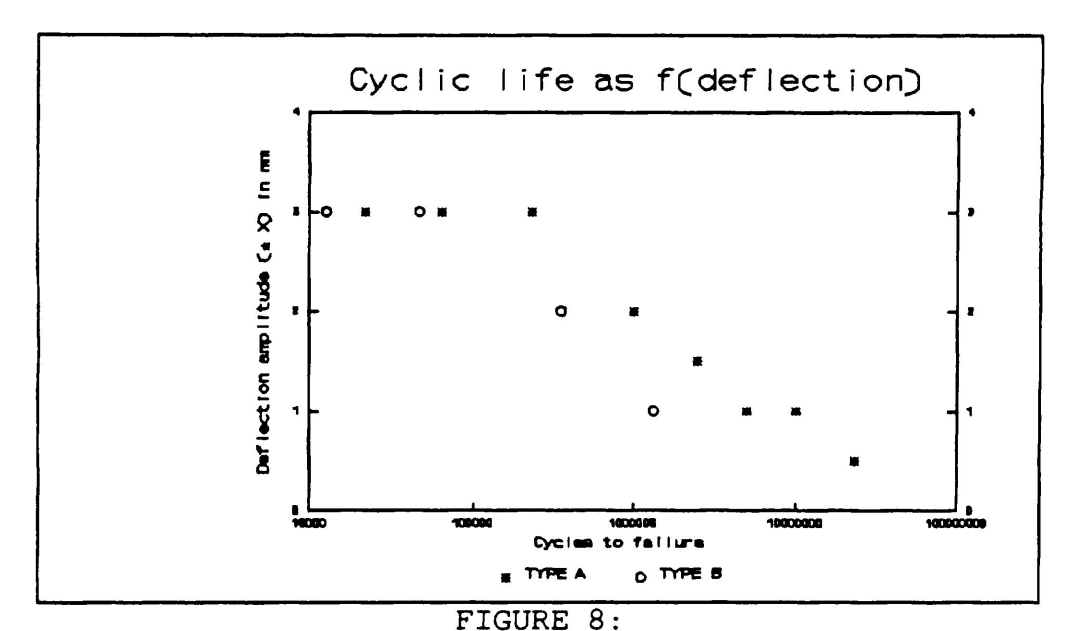
The crack at pencil #1 position (see Figure 5) had broken through the end plate. SEM examination of the fracture surface showed distinct arrest marks perpendicular to the crack propagation direction and a "black eye" at the initiation region. Evidence of fretting damage, fine particulate matter, and possibly oxidation were observed at the initiation region, resulting in the "black eye" appearance. It was not possible to obtain a correspondence between loading history and the number of arrest marks. No distinct changes could be observed in the fracture surface features in between various bands.

distinct changes could be observed in the fracture surface features in between various bands.

The crack at pencil #3 (see Figure 5) position was a partial penetration crack. Examination of the fracture surface under the SEM showed faint bands, perpendicular to the crack growth direction but with no apparent correlation to the load change history.

# 5.4 Transverse Vibration Tests-Comparison of Results

As shown in Figure 8, the effective S-N (displacement amplitude-fatigue life) curve for the two lateral tests are similar, despite having different R ( $\sigma_{\text{max}}/\sigma_{\text{min}}$ ) ratios (there is an imposed static stress on the end plate in the Type A tests as a result of the simulated hydraulic drag.) A stress analysis for the conditions used in the TYPE B tests suggested that the these specimens were somewhat more resistant to failure than similar specimens cycled axially at OHRD¹ and that the test results fit well on to the established S-N curve² for Zircaloy material. However it should be noted that conversions from deflection to stress are difficult for both test geometries.



The number of cycles to failure as a function of the half amplitude in the lateral deflection tests.

#### 6. DISCUSSION OF RESULTS

A summary table of metallurgical observations from the out-reactor simulation tests and field failures at Darlington is shown in Table 4.

TABLE 4:
A comparison of the features observed on cracks in and out of reactor

FEATURES	Field failures (Darlington)	OUT REACTOR TESTS			
		Axial Fatigue Tests (Bundle)	Lateral Vibration (type A)	Lateral Vibration (type B)	
Cycles to Failure	~1,000,000	60,000 to 130,000	25,000 to 23 million	12,000 to 1.33 million	
Crack Initiation site	Primarily at end-cap to end-plate weld notch	cap to cap to end- te plate weld plate weld		Only at end- cap to end- plate weld notch	
Endplate and/or weld failure	all failures through end plate	all failures through end plate	Amplitudes ≥ 1.5 mm: through weld. Amplitudes ≤ 1.5: through wall.	All failures through the end plate	
Primary Crack location	Int. ring/ web junction	Outer ring/ web junction	Not Applicable	Not Applicable	
Fatigue striations	.03 to 1 micron	Similar	not well defined	Similar	
Fracture surface roughness	Smooth	Smooth	Relatively Smooth	Smooth	
"Black eye" at Initiation Present Region <sup>1</sup>		Not Present	Not Present	Present	
Beach marks	Present	Not present	Not present	Present	
Fracture Surface Damage	Very little	Very little	Significant	Significant	

<sup>(1)</sup> It is not fully understood why the Black Eye was present in the variable amplitude lateral vibration or in the field failures. The varying amplitude used in the test probably induced more rubbing between the two halves of the developing crack in the initial stages of propagation.

The axial cyclic loading of bundles did not produce the pattern of cracking seen from field failures, but the crack surfaces showed a general similarity to those seen in reactor apart from the oxidation of the surfaces.

In small specimen tests at OHRD1, crack initiation occurs early in

the fatigue life and the rate of crack propagation is very slow until the crack size is at a detectable level. The axial bundle test results indicate similar progression occurs in bundle end plates although the early stages of crack growth in the axial bundle tests were likely below the UT detection limits.

Crack features and crack propagation modes similar to those induced by axial stressing were produced in the lateral deflection fatigue tests only at low amplitudes of deflection; the maximum amplitude of deflection possible for a pencil in service appears to be at the derived fatigue limit and transverse deflection above would not likely cause failure. The unique out reactor formation of the black eye feature near the point of initiation and the similarity of features to those in reactor suggest that transverse motion is a contributor to in-reactor failures. However, axial oscillation of the fuel pencils is almost certainly the prime cause of field failures. The number of cycles to failure for the same maximum load (or equivalent end plate deflection) appears to be greater in the lateral tests than in the axial tests at OHRD.

#### 7. SUMMARY

It has been demonstrated in out-reactor experiments that both transverse and axial cyclic loading can produce end plate fatigue failures similar to those seen in reactor. However, not all features of in reactor cracks could be reproduced. Axial motion seems a more likely mode of failure than lateral motion. However, the results suggest that the failures are a result of a combination of stressing conditions.

# 8. ACKNOWLEDGEMENTS

The authors would like to acknowledge the technical help of N. Preocanin, B. Burgess, B. Hargraves and C. Ropponen in carrying out the tests and the expertise in performing ultrasonic inspection at OHRD under the direction of M. Dolbey. The authors would also like to acknowledge M. Gacesa who defined the rationale for the single element lateral deflection tests and provided analytical comment and encouragement during the course of the work.

#### REFERENCES

- 1. E.T.C. Ho, G.K. Shek, M.L. Vanderglas and M. Leger "Development of Fatigue Failure Criteria for Darlington Fuel Bundle Endplates", to be presented at the CNS. 1992 Conference
- 2. W.J. O'Donnell and B.F. Langer, "Fatigue Design Basis for Zircaloy Components", Nuclear Science and Engineering, 20, 1 (1964).